A regulatory network of T-box genes and the *even-skipped* homologue *vab-7* controls patterning and morphogenesis in *C. elegans*

Roger Pocock[1], Julie Ahringer[2], Michael Mitsch[2], Sara Maxwell[1] and Alison Woollard[1,*]

[1]Genetics Unit, Department of Biochemistry, University of Oxford, South Parks Road, Oxford OX1 3QU, UK
[2]Wellcome Trust/Cancer Research UK Gurdon Institute, University of Cambridge, Tennis Court Road, Cambridge CB2 1QR, UK
*Author for correspondence (e-mail: woollard@bioch.ox.ac.uk)

Accepted 3 February 2004

Development 131, 2373-2385
Published by The Company of Biologists 2004
doi:10.1242/dev.01110

Summary

T-box genes form a large family of conserved transcription factors with diverse roles in animal development, but so far functions for only a few have been studied in detail. Here we show that four *Caenorhabditis elegans* T-box genes and the *even-skipped*-like homeobox gene *vab-7* function within a regulatory network to control embryonic patterning and morphogenesis. *tbx-8* and *tbx-9* have functionally redundant roles in the intercalation of posterior dorsal hypodermal cells, in muscle cell positioning and in intestinal development. Inhibiting *tbx-9* alone using RNA interference (RNAi) produces worms that have a thickened, 'bobbed tail' phenotype, similar to that seen in mutants of *vab-7*, which itself has been shown to pattern posterior muscle and hypodermal cells. In support of the view that these genes function in the same pathway, we find that *tbx-8* and *tbx-9* are both necessary and sufficient for *vab-7* expression. In addition, a third T-box gene, *tbx-30*, acts to repress *vab-7* expression in the anterior of embryos. We further show that *vab-7* itself represses the T-box gene *mab-9* in posterior cells. Thus, during posterior patterning in *C. elegans*, there are multiple interactions between T-box genes and the *vab-7* homeobox gene. Evolutionary parallels in other organisms suggest that regulatory interactions between T-box genes and *even-skipped* homologues are conserved.

Key words: *Caenorhabditis elegans*, T-box genes, Dorsal intercalation, *evenskipped*

Introduction

T-box genes are a large family of transcriptional regulators unified by a conserved DNA binding, or T, domain that have important, yet diverse roles in patterning animal development (reviewed by Papaioannou, 2001). Mouse mutations in T-box genes such as *Brachyury* and *Tbx6* are associated with notochord and mesoderm, or neural tube defects, respectively (Herrmann, 1995; Chapman and Papaioannou, 1998), and chick *Tbx4* and *Tbx5* have roles in limb specification (reviewed by Simon, 1999). In *Xenopus*, *Brachyury* (*Xbra*) is required for the development of mesoderm (Conlon et al., 1996), while *VegT* is required for induction of mesoderm and endoderm (Kofron et al., 1999; Zhang et al., 1998). The *Drosophila Brachyury* homologue *brachyenteron* (*byn*), or *Trg*, functions in the formation of hindgut and posterior mesoderm (Kispert et al., 1994; Singer et al., 1996; Kusch and Reuter, 1999), while *optomotor blind* (*omb*) is necessary for the development of anterior sensory structures such as the eye (Pflugfelder and Heisenberg, 1995). In addition, several T-box genes are associated with human developmental abnormalities, including Holt-Oram syndrome (Basson et al., 1999), Ulnar-Mammary syndrome (Bamshad et al., 1999) and X-linked cleft palate (Braybrook et al., 2001), further highlighting the critical functions of members of this gene family.

All T-box proteins tested so far appear to bind to the same consensus DNA binding site (Kispert et al., 1995; Muller and Herrmann, 1997). T-box genes can be divided into several subfamilies based on sequence comparisons, and some subfamilies are highly conserved across a wide range of phyla from *Caenorhabditis elegans* to humans (Papaioannou, 2001). The completed *C. elegans* genome sequence predicts 20 T-box genes in *C. elegans*, more than in any other species analysed so far, but functions for only two, *mab-9 and mls-1*, have been studied in detail (Woollard and Hodgkin, 2000; Kostas and Fire, 2002). Most of the *C. elegans* T-box genes appear to be highly diverged from those found in other species, with only four genes having obvious counterparts in other organisms (Papaioannou, 2001). *mab-9* is a member of the Tbx20 subfamily (Papaioannou, 2001) and is required for cell fate specification in the developing hindgut and for proper motor neuron function (Woollard and Hodgkin, 2000; Huang et al., 2002). *mls-1*, related to the Tbx1 subfamily, is necessary for correct muscle cell fate determination (Kostas and Fire, 2002). Two other T-box genes with orthologues in other organisms, *F21H11.3* (*tbx-2*), a member of the Tbx2 subfamily, and *ZK328.6* (*tbx-7*), related to the ascidian gene *T2* (Papaioannou, 2001), have not yet been characterised. Unlike other species tested so far, *C. elegans* does not have a recognisable *Brachyury* orthologue.

We have taken a reverse genetic approach to analysing T-box gene function in *C. elegans*. We used RNA interference (RNAi) to survey loss of function phenotypes for T-box genes

and found that RNAi of *tbx-9* resulted in a phenotype similar to that of *vab-7* mutants. *vab-7* is a homologue of the *Drosophila* homeobox gene *even-skipped* (*eve*), required for posterior patterning of muscle and hypodermal cells in *C. elegans* (Ahringer, 1996); *eve* homologues also have roles in posterior development in several other species (Brown et al., 1997; Joly et al., 1993). We find that *tbx-9*, *vab-7* and three other T-box genes act within a regulatory pathway important for embryonic development, with *vab-7* functioning both upstream and downstream of T-box genes to regulate posterior patterning.

Materials and methods

Strains and *C. elegans* maintenance

All *C. elegans* strains were derived from the wild-type Bristol strain N2. Routine maintenance of worms and genetic manipulations were performed as described (Sulston and Hodgkin, 1988).

RNAi

PCR primers, including T7 or T3 RNA polymerase promoter sites, were designed to be specific to the gene to be silenced and to amplify typically 500-900 bp of mostly exonic sequence. dsRNA was synthesised directly from gel-purified PCR product as previously described (Fire et al., 1998) and injected into young N2 adult hermaphrodites at a concentration of ~1 mg/ml. Injected worms were transferred to fresh plates 6 hours following injection and thereafter every 10-14 hours for 3 days.

RT-PCR

One hundred mixed-stage embryos were isolated from the progeny of wild type, *tbx-8(RNAi)* and *tbx-9(RNAi)* hermaphrodites. Total RNA was extracted using the RNeasy® RNA extraction kit (Qiagen, Crawley, UK). RT-PCR amplification of *tbx-8*, *tbx-9* and *ama-1* (control) mRNA was carried out on these total RNA samples using Superscript™ One-Step RT-PCR with Platinum® *Taq* (Invitrogen, Paisley, UK). Gene specific RT-PCR oligos (designed to anneal to either side of an intron to enable DNA and RNA amplification to be distinguished and to give RT-PCR products of around 200 bp) were as follows: *tbx-8* (F cgtctt-gtcacttctgttcg, R ccctctcggaatccttggc), *tbx-9* (F agtaacggcttaccagaacc, R tggggactgtgagttgctgc), *ama-1* (F ttccaagcgccgctgcgcattgtctc, R cagaatttccagcactcgaggagcgga).

Transgenic worms

Plasmids were injected into the syncytial gonad of young adult hermaphrodite worms at concentrations of 1-50 ng/μl as described (Mello and Fire, 1995). Co-transformation markers were either *rol-6* (plasmid pCes1943, gift of Diana Janke, University of British Columbia), in which case Rol progeny from N2 injected worms were picked and stable lines selected, or *unc-119*$^{(+)}$ (plasmid pDP#MM016β), in which case non-Unc progeny from *unc-119 (ed3)* injected worms were selected. Where appropriate, integrated lines were generated by X-ray mutagenesis as described previously (Mello and Fire, 1995). Integrated lines were outcrossed several times prior to analysis.

GFP reporter constructs

GFP fusions were made using pPD vectors kindly supplied by the Fire Lab (Carnegie Institute of Washington). All constructs were verified by sequencing. To make a *tbx-8::GFP* fusion, a PCR fragment (oligos F aaaactgcagaccggtttggcagctacac, R aaaactgcaggccattgatttc ctgctcaatatc) containing the entire coding and 5′ intergenic region minus the stop codon (7.7 kb) was first inserted into pBSKS^{+} (Stratagene) using *Pst*I and then sub-cloned into pPD95.77 to make an in-frame GFP translational fusion (plasmid pAW232). Several transgenic lines were generated carrying this construct using 20-50 ng/μl DNA, giving very similar expression patterns. The strain described in this report is AW27 (*ouEx12*[pAW232 + pCes1943]). To make a *tbx-9::GFP* fusion, a PCR fragment (oligos F aaaactgcaggattcaatcaaaacgggc, R aaaactgcaggcaccaacaatatcaatatcttc) was cloned directly into pPD95.75 using *Pst*I to make an in-frame translational fusion (plasmid pJA57). Several transgenic lines were generated carrying this construct, using 1 ng/μl DNA (higher concentrations were found to be toxic). Transgenic lines gave similar expression patterns. The strain described in this report is AW22 (*unc-119 (ed3); ouEx8* [pJA57 + pDP#MM016β]). A *vab-7::GFP* reporter construct was made by cloning GFP in-frame into the *Sph*I site of exon 1 of the *vab-7* genomic rescuing construct pJA17 (14 kb), to generate the translational fusion construct pJA64, which was injected at a concentration of 20-50 ng/μl. This construct gave the same expression pattern in transgenic worms as the *lacZ* reporter and in-situ hybridisations previously described (Ahringer, 1996). The *vab-7::GFP* transgenic strain described in this report is AW23 (*unc-119 (ed3); ouEx9* [pJA64 + pDP#MM016β]). The integrated *mab-9::GFP* strain (*eIs34*) used in this study has been described previously (Woollard and Hodgkin, 2000). This was crossed into *vab-7(e1562)* to give the strain AW24. The integrated *pal-1::GFP* strain (*ctIs33*) used in this study was a gift from Lois Edgar (University of Colorado, Boulder). The *elt-2::GFP* reporter strain (*wIs81[elt-2::GFP;pRF4(rol-6)*]) was a gift from Joel Rothman (University of California, Santa Barbara).

Heat-shock constructs

Two *hsp-16* driven *tbx-9* constructs were made. pJA50 consists of the *tbx-9* full-length cDNA (*Xba*I-*Kpn*I insert from cDNA clone pYK337c3) cloned into pPD49.78 (*hsp16-2* driven), and pJA52 consists of the same cDNA insert cloned into pPD49.83 (*hsp16-41* driven). A transgenic line was derived containing both *hsp16::tbx-9* constructs, *weEx41* [pJA50 + pJA52 + pRF4 (*rol-6*)]. An integrated strain was subsequently derived from this, *weIs8* (strain JA1286). A similar approach was taken to construct a strain (JA1284, *weIs6*) containing an integrated copy of an extrachromosomal array containing *hsp16-2* driven (pJA49) and *hsp16-41* driven (pJA51) *tbx-8* cDNAs, derived from the cDNA clone pYK325e8. Integrated heat-shock driven *tbx-8* and *tbx-9* strains were then crossed into an *unc-119 (ed3)* background and injected with the *vab-7::GFP* construct described above (pJA64) together with *unc-119*$^{(+)}$ to give the strains AW26 (*unc-119(ed3); weIs8 (hsp-16::tbx-9 + rol-6); ouEx11* [pJA64 + pDP#MM016β]) and AW41 (*unc-119(ed3); weIs6 (hsp-16::tbx-8 + rol-6); ouEx14* [pJA64 + pDP#MM016β]). Non Unc, Rol progeny were selected in each case. Adult hermaphrodite worms were subsequently heat shocked at 33°C for 45 minutes and then incubated at 20°C for 2 hours and embryos dissected for examination.

Site-directed mutagenesis

A 4.3 kb *Pac*I-*Pfl*MI subclone (plasmid pAW223) of the *vab-7::GFP* reporter pJA64 containing the putative T-box binding sites to be mutated was used for site-directed mutagenesis. Site B was mutated first (see legend to Fig. 8) to generate plasmid pAW224 using the Stratagene Quickchange kit and protocols. Mutagenesis PCR oligos were as follows: F gtacgcctcattgatgtaatgtaaaagagatgtg R catgcggagtaactacattacatttttctctacac. Site A was subsequently mutated to generate pAW226, in which both putative T-box binding sites were mutated. PCR oligos were as follows: F cgagcggaaaagatgta-tttgaaccttcc R gctcgccttttctaca taaacttggaagg. The mutated *Pac*I-*Pfl*MI fragment was then re-inserted into the *vab-7::GFP* reporter construct pJA64 to generate the plasmid pAW231, a *vab-7::GFP* reporter in which both putative T-box binding sites in the *vab-7* regulatory region were mutated into sites that would not be expected to permit T-box proteins to bind (Sinha et al., 2000). Transgenic lines were generated using this construct that gave similar expression patterns. The

transgenic line described in this report is AW28 (*ouEx13* [pAW231 + pCes1943]).

Antibody staining

To verify that the cells expressing *tbx-8* and *tbx-9::*GFP fusions were the cell types they appeared to be by morphology and position, the following antibodies were used and co-localisation was assessed: a GFP antibody (chicken monoclonal from Chemicon, Hampshire, UK) for visualising TBX-8 and TBX-9::GFP fusions, LIN-26 antibody (gift from M. Labouesse, Strasbourg), which stains all hypodermal cells, and mouse mAb NE8/4C6.3, which stains the outlines of body wall muscle cells (Goh and Bogaert 1991). Secondary antibodies were FITC anti-chicken or Texas Red anti-mouse (Jackson Immunoresearch, Pennsylvania, USA). Immunostaining experiments were performed as follows: embryos were placed on poly-lysine coated slides, squashed under a coverslip and frozen on dry ice for 20 minutes. After freezing, the coverslip was flicked off and slides placed in methanol for 20 minutes at room temperature, washed with PBS for 5 minutes and PBS + Tween (0.2%) for 10 minutes. Primary antibodies were incubated overnight at 4°C in PBS+Tween. After washing, secondary antibodies were incubated for 1-2 hours at room temperature. Samples were mounted in mowiol.

Results

RNAi of *tbx-8* and *tbx-9* reveals overlapping functions in embryonic development

A phylogenetic tree of *C. elegans* T-box genes together with representative members of each of the defined T-box subfamilies found in other organisms (Papaioannou, 2001) is shown in Fig. 1A. This illustrates the high degree of divergence of most of the *C. elegans* T-box genes, with the exception of the four genes discussed above. There are several putative paralagous pairs of T-box genes in *C. elegans*, which may be the result of recent gene duplications.

A survey of *C. elegans* T-box gene function by RNAi has revealed obvious phenotypes in only a few cases (Maxwell, Aslam and Woollard, unpublished observations; Ahringer, unpublished observations). The *tbx-9(RNAi)* phenotype consists of a characteristic swelling of the hermaphrodite tail hypodermis, giving a 'bobbed tail' appearance highly reminiscent of the tail phenotype seen in *vab-7(e1562)* animals (Fig. 2). This phenotype is not very penetrant in N2 animals (~10%). When RNAi experiments were conducted in the *rrf-3* strain, which is more sensitive to RNAi (Simmer et al., 2002), the penetrance of *tbx-9(RNAi)* phenotypes was increased: 15-25% of the progeny of *rrf-3* dsRNA injected hermaphrodites had a *vab-7*-like bobbed tail and, in addition, 10-15% of progeny had other morphological defects, including dorsal hypodermal bulges in the midbody and posterior region (data not shown).

The phylogenetic tree presented in Fig. 1 suggests that *tbx-8* and *tbx-9* may be paralogous. The two proteins are 59% identical in their T-box domains and are located only 3.75 kb apart on chromosome III (map position 2.41). They are divergently transcribed and thus may share common 5′ regulatory regions (Fig. 1B). RNAi of *tbx-8* revealed no obvious abnormalities, either in N2 or *rrf-3* animals (Fig. 2B and data not shown). To test the efficacy of RNAi for both *tbx-8* and *tbx-9*, we assayed *tbx-8* and *tbx-9* mRNA levels in embryos by RT-PCR and found that both mRNAs were undetectable following injection of the corresponding dsRNA (Fig. 2G). We also found that *tbx-8* and *tbx-9* RNAi abolished the GFP signals of *tbx-8::GFP* and *tbx-9::GFP* transgenic worms, respectively (data not shown).

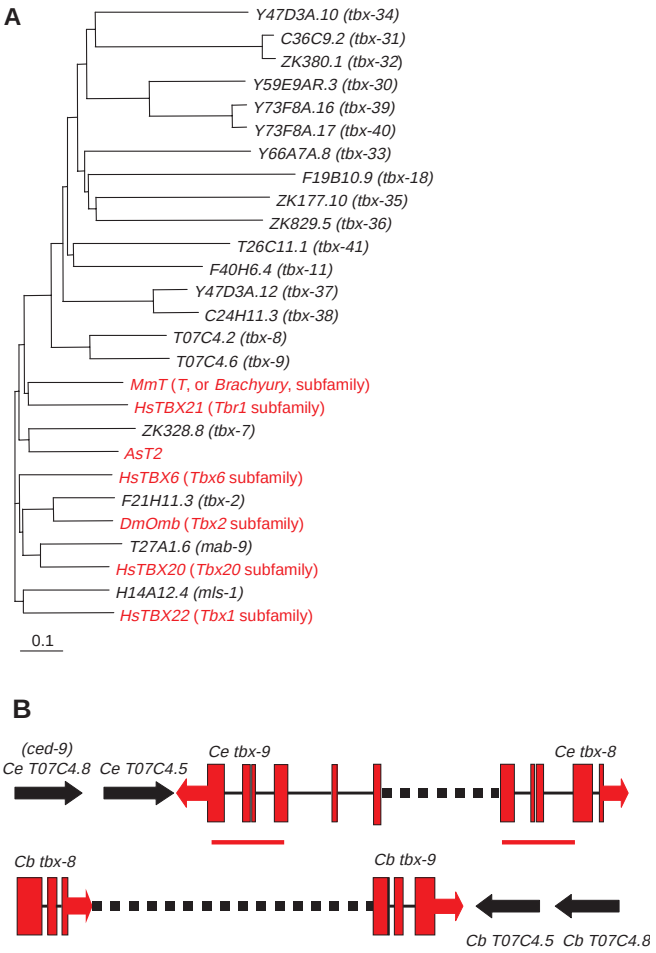

Fig. 1. Phylogenetic analysis of T-box genes. (A) Phylogenetic tree. T-box domain amino acid sequences of all *C. elegans* T-box genes and representative members of the defined T-box subfamilies found in other organisms (Papaioannou, 2001) were aligned using ClustalW accessed via the European Bioinformatics Institute (EBI, http://www.ebi.ac.uk/). The alignment was subjected to Phylip analysis using the same EBI interface and Phylip outputs were interpreted using the tree drawing programme TreeView. Non-*C. elegans* genes are in red. Species abbreviations are as follows: *As*, ascidian; *Dm*, *Drosophila melanogaster*; *Hs*, *Homo sapiens*; *Mm*, *Mus musculus*. New *C. elegans* gene names (*tbx-30-41*) have been approved by the Caenorhabditis Genetics Centre (CGC). (B) Genomic organisation of *tbx-8* and *tbx-9* (and neighbouring genes) in *C. elegans* and *C. briggsae*. *Ce-tbx-8* and *Ce-tbx-9* are transcribed in opposing directions (arrows), whereas *Cb-tbx-8* and *Cb-tbx-9* are transcribed in the same direction (arrows). The thick dotted line represents the intergenic region. *Ce-tbx-8* and *Cb-tbx-8* are 73% identical throughout their T-box domains. *Ce-tbx-9* and *Cb-tbx-9* are 56% identical. There is evidence of a local chromosome inversion in *C. briggsae* compared with *C. elegans*, which extends for several genes to the right of *Cb-tbx-9* (neighbouring region not drawn to scale). Red bar denotes the T-box domain of *Ce-tbx-8* and *Ce-tbx-9* (59% identical).

To test whether *tbx-8* and *tbx-9* have overlapping functions, double RNAi experiments were performed. Silencing of both genes simultaneously in N2 animals gave rise to 100% embryonic or early larval lethality (50-60% embryonic arrest, 40-50% L1 arrest, *n*=130), with gross morphological defects in

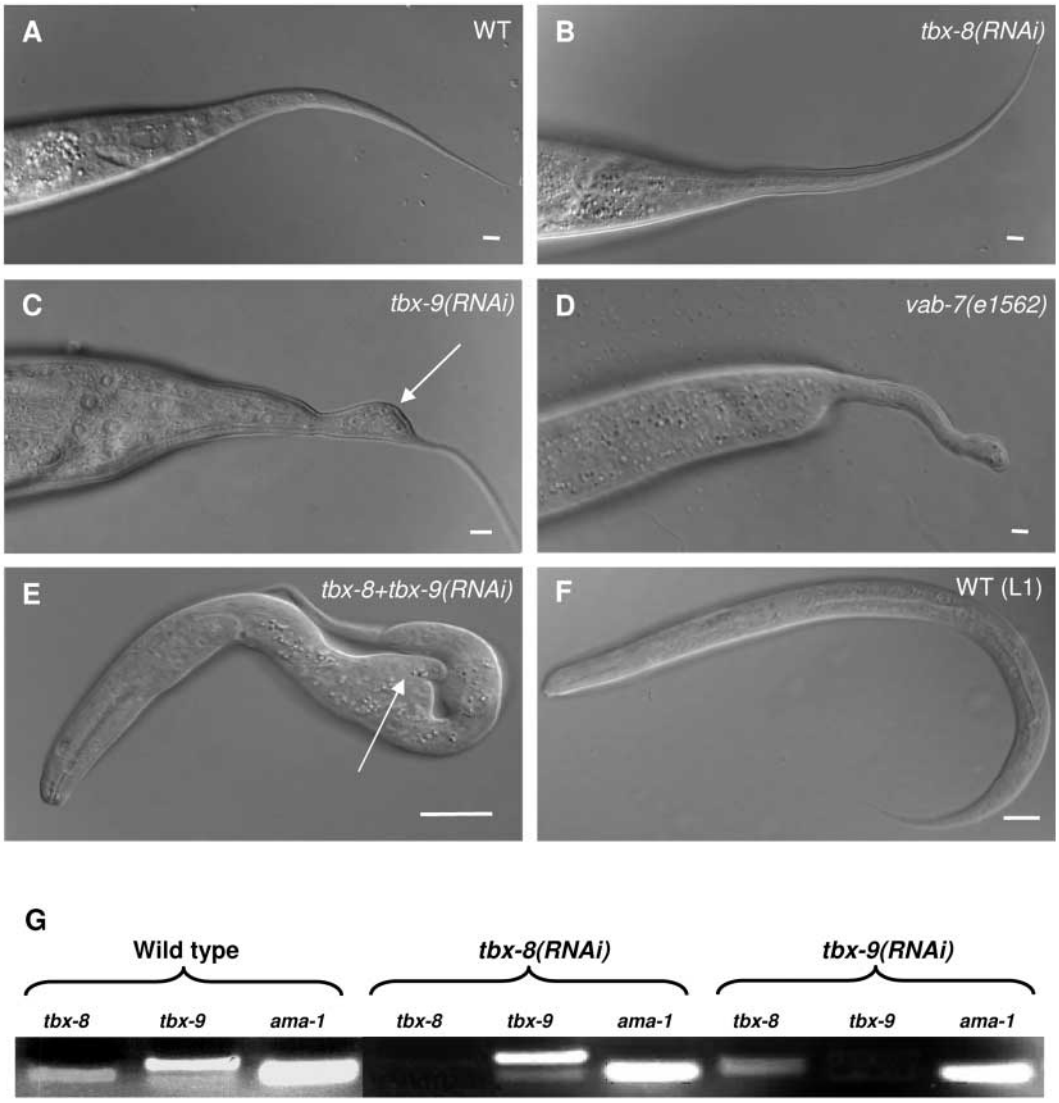

Fig. 2. RNA interference (RNAi) phenotypes of *tbx-8* and *tbx-9*. (A) Wild-type adult hermaphrodite tail whip. (B) Tail region of adult hermaphrodite progeny of wild-type worm injected with dsRNA corresponding to *tbx-8*. These worms are indistinguishable from wild type. (C) Tail region of *tbx-9(RNAi)* worms. The adult hermaphrodite tail is thickened (arrow) and often has a 'bobbed tail' appearance. (D) Tail region of adult hermaphrodite *vab-7(e1562)* animal. The tail is similar in appearance to that in (C). (E) L1 larvae from hermaphrodite mother co-injected with *tbx-8* and *tbx-9* dsRNA. In addition to thickening of the tail, these animals display gross midbody and posterior morphological abnormalities, often with large dorsal bulges (arrow). Most die as unelongated embryos or short L1s. (F) Wild-type L1. Scale bars, 10 μm. Posterior is to the right and dorsal is up in all panels. (G) RT-PCR analysis of *tbx-8* and *tbx-9* transcripts in wild-type worms and those subjected to *tbx-8* and *tbx-9* RNAi. *ama-1* was chosen as a suitable control, as mRNA would be expected to be constant throughout. For each gene, primers were chosen to specifically amplify mRNA of approximately 200 bp (see Materials and methods). Results were identical for three separate experiments.

the midbody region and posterior (Fig. 2E, Fig. 4). There was a failure of body elongation, and hatched animals had large dorsal bulges in the hypodermis (Fig. 2E). We compared phenotypes observed in double RNAi experiments with those of a *tbx-8* knockout allele (*ok656*, a presumed null allele available from the *C. elegans* Knockout Consortium, Oklahoma, USA), which had been subjected to *tbx-9* RNAi and found that they were identical: *tbx-8(ok656); tbx-9(RNAi)* animals also arrest as embryos or early larvae in similar proportions (53% embryonic arrest, 46% L1 arrest, n=220), with identical morphological defects (data not shown). This demonstrates the efficacy of silencing *tbx-8* and *tbx-9* simultaneously by double RNAi. *tbx-8(ok656)* worms, like *tbx-8(RNAi)* animals, have no obvious defects on their own (data not shown).

Co-silencing of *tbx-8* and *tbx-9* causes defects in embryonic dorsal intercalation and in hypodermal and muscle cell positioning

The dorsal bulges displayed by *tbx-8/tbx-9(RNAi)* animals suggested that hypodermal morphogenesis might have been affected. In wild-type embryos, the two rows of dorsal hypodermal cells, born around 240 minutes after first cleavage, intercalate into a single dorsal row around 290-340 minutes (Fig. 3A). During dorsal intercalation, dorsal hypodermal cells become wedge-shaped, with their pointed ends oriented towards the dorsal midline. The pointed tips of these cells interdigitate contralaterally and elongate so that the advancing edges eventually contact the opposing lateral hypodermal (seam) cells, which flank the dorsal hypodermis (Fig. 3A). Migration of dorsal nuclei follows behind the extending cell tips, so that the nuclei end up close to the lateral seam cells. The hypodermis then extends ventrally, spreading to enclose the embryo, with ventral hypodermal cells eventually sealing up the ventral pocket by a 'purse-string' mechanism at 310-360 minutes. Dorsal hypodermal cells subsequently undergo fusion to form a syncytium, and circumferential contraction within the hypodermis causes a fourfold elongation of the embryo (360-600 minutes). The rearrangement and movements

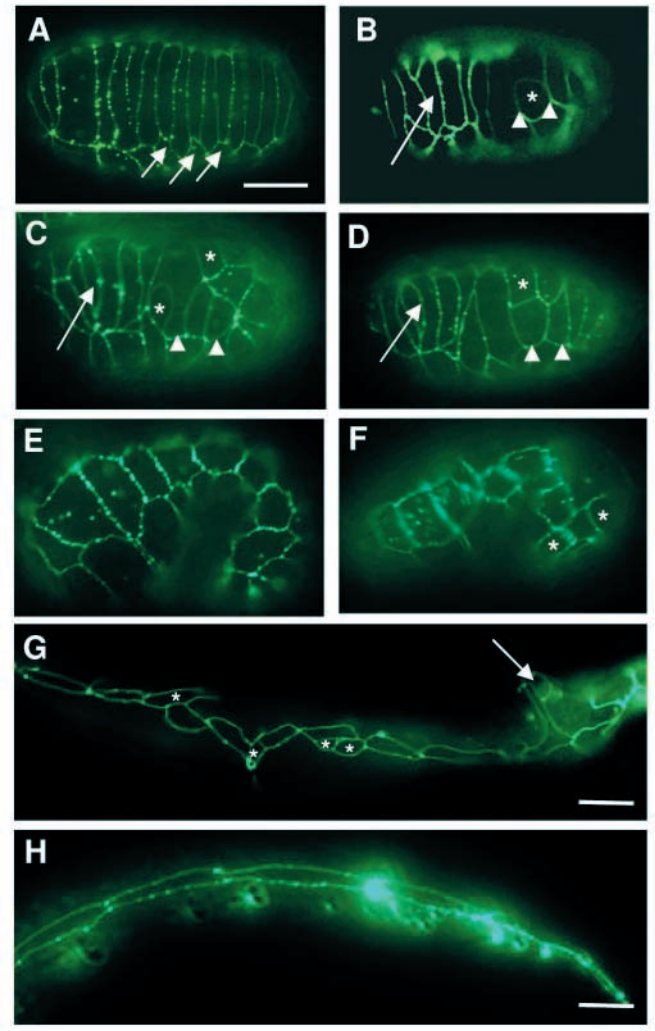

Fig. 3. Hypodermal defects in *tbx-8/tbx-9(RNAi)* animals. The arrangement of hypodermal cells in embryos and L1 larvae has been visualised using the *ajm-1::GFP* reporter. (A-D) Dorsal view. (A) Wild-type embryo around 300 minutes following first cleavage. The two rows of dorsal hypodermal cells born 1 hour previously have intercalated into a single row and their advancing edges have come into contact with the opposing lateral hypodermal cells (arrows). (B-D) *tbx-8/tbx-9(RNAi)* embryos at approximately the same stage. Dorsal hypodermal cells are clearly disorganised. In most embryos dorsal intercalation begins relatively normally at the anterior (B-D, arrow) but does not proceed normally in the midregion or posterior (B-D, arrowheads). In these embryos, dorsal intercalating cells that are not the appropriate wedge-shape can be seen (B-D, asterisks), and many cells do not extend contralaterally in the correct way. Dorsal intercalation often arrests at this point, the same misarranged cells being observable at least 1 hour later. (E-H) Arrangement of lateral hypodermal (seam) cells in *tbx-8/tbx-9(RNAi)* embryos and L1 larvae. (E) Wild-type embryo beginning elongation, lateral view. A linear row of seam cells can be seen. (F) *tbx-8/tbx-9(RNAi)* embryo, same stage and view. The lateral row of cells is interrupted, with some cells being pinched out of line (asterisks). (G) *tbx-8/tbx-9(RNAi)* animal that has survived to hatching; some seam cells are pinched out of line (asterisks) and are misshapen at the site of the dorsal bulge (arrow). Animals are much shorter than they should be in L1 (compare with (H) wild type, posterior half only of animal, same scale). Posterior is to the right in all panels. Scale bars, 10 μm.

of groups of hypodermal cells during embryonic development is instrumental in setting the shape of the worm (reviewed by Chin-Sang and Chisholm, 2000; Simske and Hardin, 2001).

To analyse hypodermal cell positions and migrations, we used the *ajm-1::GFP* (pka *jam-1::GFP*) reporter (strain SU93), which marks adherens junctions, allowing visualisation of the outlines of hypodermal cells (Mohler et al., 1998). In *tbx-8/tbx-9(RNAi)* embryos, dorsal intercalation is defective (Fig. 3). In these embryos, dorsal intercalation is relatively normal at the anterior end of the embryo but fails to complete towards the posterior (Fig. 3B-D). Some of the cells appear square, or even rounded, rather than wedge-shaped, and intercalation appears to arrest at this point (Fig. 3B-D). Observation of the same embryos 90 minutes later showed that dorsal intercalation does not proceed beyond this stage (data not shown). No obvious defects in ventral enclosure were evident (data not shown); however, defects in the arrangement of lateral hypodermal (seam) cells could be seen. In wild-type embryos, lateral hypodermal cells form two linear rows with 10 cells on each side of the embryo (Fig. 3E). In *tbx-8/tbx-9(RNAi)* embryos, lateral rows are interrupted, with one to four cells pinched out of line (Fig. 3F). However, seam cell number is not affected (data not shown). This misalignment of seam cells can also be seen in those RNAi worms that survive to hatching (Fig. 3G). *tbx-8/tbx-9(RNAi)* embryos fail to elongate properly and die either as late-stage embryos (50-60%) or misshapen, short L1 larvae (40-50%), with large bulges typically, though not exclusively, on the dorsal side (Fig. 2E).

Muscle cells are also affected in *tbx-8/tbx-9(RNAi)* animals. In wild-type animals, body wall muscles are present as two regular rows on the dorsal and ventral sides of the animal and can be visualised using *hlh-1::GFP* or *myo-3::GFP* transgenic markers. In *tbx-8/tbx-9(RNAi)* embryos and hatched larvae, these rows are not regular. Muscles are often seen out of line and rows are sometimes broken down completely, with muscle cells being bunched together laterally (Fig. 4B,D,F). The overall number of muscle cells, as assessed by counting nuclei expressing the muscle marker *hlh-1::GFP* at the 2-fold stage, is unchanged (wild type, 58 (n=22), *tbx-8/tbx-9(RNAi)*, 58 (n=17)), suggesting that this is a positioning, rather than a cell fate commitment, defect. The earliest observable muscle-positioning defect was seen around the 400 cell stage, as dorsal hypodermal intercalation was proceeding (Fig. 4B). We cannot exclude the possibility, therefore, that muscle-positioning defects are caused by abberant dorsal hypodermal morphogenesis, rather than being a cell autonomous defect. Likewise, it is possible that some of the hypodermal defects observed were a secondary consequence of muscle-positioning defects. However, it is known from ablation experiments that dorsal hypodermal intercalation proceeds normally in the absence of the underlying muscle tissue (Heid et al., 2001), consistent with our view that hypodermal defects in *tbx-8/tbx-9(RNAi)* embryos are unlikely to be a secondary consequence of muscle-positioning defects. Furthermore, bulges on the surface of *tbx-8/tbx-9(RNAi)* animals that survived to L1 were always correlated with gross disorganisation of hypodermis, while some bulges did not contain muscle cells (data not shown), suggesting that hypodermal defects were the primary cause.

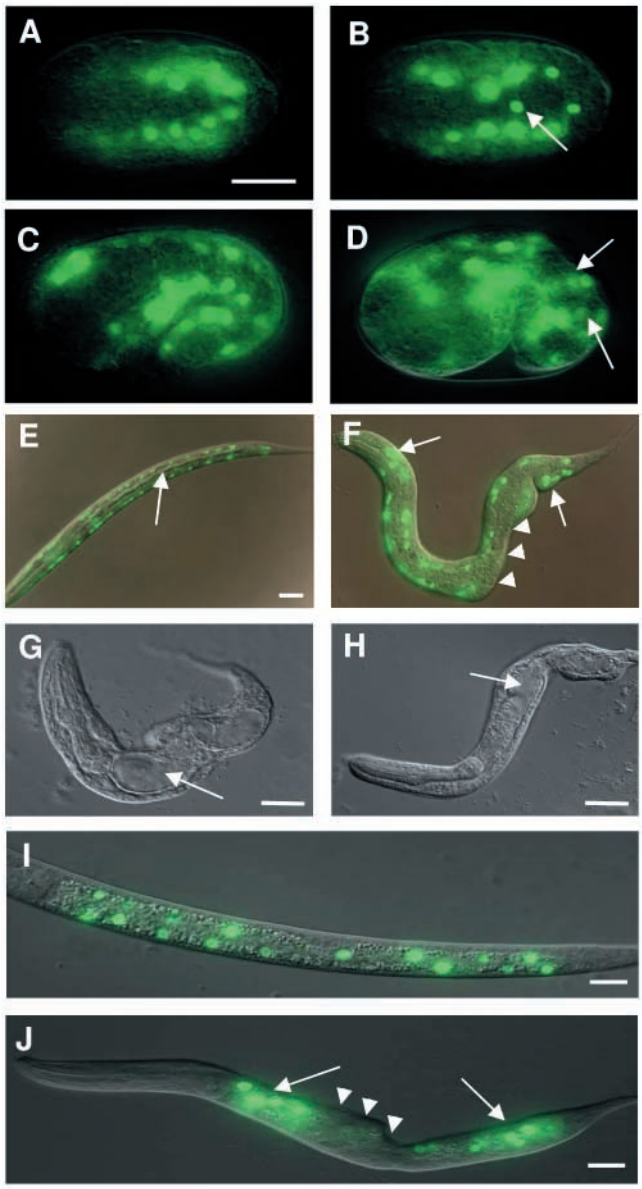

Fig. 4. Muscle and intestinal defects in *tbx-8/tbx-9(RNAi)* animals. (A-D) Transgenic embryos carrying an *hlh-1::GFP* body wall muscle reporter. Body wall muscle nuclei are green. (A-B) Embryos around the 400-cell stage. (A) Wild type, dorsal view. Two rows of muscle cells (one on the right and one on the left side of the embryo) are visible at this stage. (B) *tbx-8/tbx-9(RNAi)* embryo. Some muscle cells are not in regular rows (arrow). (C-D) Embryos at the 1.5-fold stage. (C) Wild type, left lateral view. Muscles have split into dorsal and ventral rows on each side of the embryo. One dorsal and one ventral row can be seen in this focal plane. (D) *tbx-8/tbx-9(RNAi)* embryo. There is no clear separation of dorsal and ventral rows, especially at the posterior (arrows). (E-F) transgenic animals carrying a *myo-3::GFP* body wall muscle reporter. (E) Dorsal view of wild-type L1, showing two of the four rows of muscle nuclei; two ventral rows are not visible in this focal plane. (F) Muscle nuclei in *tbx-8/tbx-9(RNAi)* animals. Instead of lying in straight rows, nuclei are often bunched (arrows), and there are gaps in the row (arrowheads). (G-J) Intestinal defects in *tbx-8/tbx-9(RNAi)* animals. (G-H) *tbx-8/tbx-9(RNAi)* animals that have survived to hatching. The intestine has severe morphological defects with the gut lumen being highly distended (arrows). In comparison, a wild-type gut lumen is visible in (E) (arrow). (I-J) Transgenic worms carrying an *elt-2::GFP* intestinal cell reporter. Intestinal nuclei are green. (I) Wild-type L1 showing the positions of 16 of the 20 intestinal nuclei (the other four are out of focus). (J) *tbx-8/tbx-9(RNAi)* L1 worm. The intestinal nuclei are out of position, often being bunched together at either end of the intestine (arrows) and missing from the middle (arrowheads). Counting reveals that all nuclei are usually present, however. Posterior is to the right in all panels. Scale bars, 10 μm.

Intestinal defects in *tbx-8/tbx-9(RNAi)* worms

tbx-8/tbx-9(RNAi) animals that survived to hatching had abnormal gut morphology (Fig. 4G,H,J). Using an *elt-2::GFP* intestinal cell marker, we examined the number and positions of intestinal nuclei in wild-type and *tbx-8/tbx-9(RNAi)* worms. We found that the number of intestinal cells was unchanged at the 1.5-fold stage (wild type, 19 (n=14), *tbx-8/tbx-9(RNAi)*, 19 (n=22)). These cells were correctly positioned at this stage (data not shown) but in hatched *tbx-8/tbx-9(RNAi)* animals intestinal cells were mispositioned (Fig. 4J compared with Fig. 4I). This suggests a potential role for *tbx-8* and *tbx-9* in intestinal morphogenesis, although it may be that *tbx-8* and *tbx-9* do not have a direct role in intestinal cell positioning; positioning defects during late embryogenesis could be a consequence of aberrant morphogenesis. Likewise, it is possible that intestinal defects in *tbx-8/tbx-9(RNAi)* worms are a secondary consequence of defective embryonic elongation.

Domains of expression of *tbx-8* and *tbx-9*

The expression patterns of *tbx-8* and *tbx-9* GFP translational fusions are shown in Fig. 5. *tbx-8* and *tbx-9* are both expressed in three different cell types in the embryo, gut, muscle and hypodermis, in a largely overlapping pattern. In all cases expression was found to be nuclear, as would be expected for putative transcription factors. The earliest embryonic expression of both *tbx-8* and *tbx-9* was detected in the E lineage gut cell precursors Ea and Ep at the beginning of gastrulation (~100 minutes after first cleavage) (Fig. 5A,B). Expression was seen in the direct descendents of Ea and Ep but was not obvious later in E lineage nuclei (data not shown). Although the expression of *tbx-8* and *tbx-9* in intestinal cells is consistent with a possible role for *tbx-8* and *tbx-9* in gut development, it is not clear how the early gut expression of *tbx-8* and *tbx-9* in gut cell precursors relates to the intestinal defects seen in *tbx-8/tbx-9(RNAi)* worms, which only become apparent later in embryogenesis, as discussed above.

tbx-8 and *tbx-9* were subsequently expressed in muscle and hypodermal cells (Fig. 5C-I). The expression of both *tbx-8* and *tbx-9* was stronger in dorsal hypodermal nuclei, which were just starting to intercalate, compared with those at the anterior, which were intercalated, or those at the posterior, which had yet to intercalate (Fig. 5E-G). This is particularly evident in embryos that have been co-stained with LIN-26 and GFP antibodies (Fig. 5I) and is consistent with a role for *tbx-8* and *tbx-9* in the process of dorsal intercalation, as suggested by the phenotypic analysis presented above. Expression of *tbx-8* and *tbx-9* could also be seen in dorsal hypodermal nuclei undergoing contralateral migration following cellular intercalation (data not shown), and in

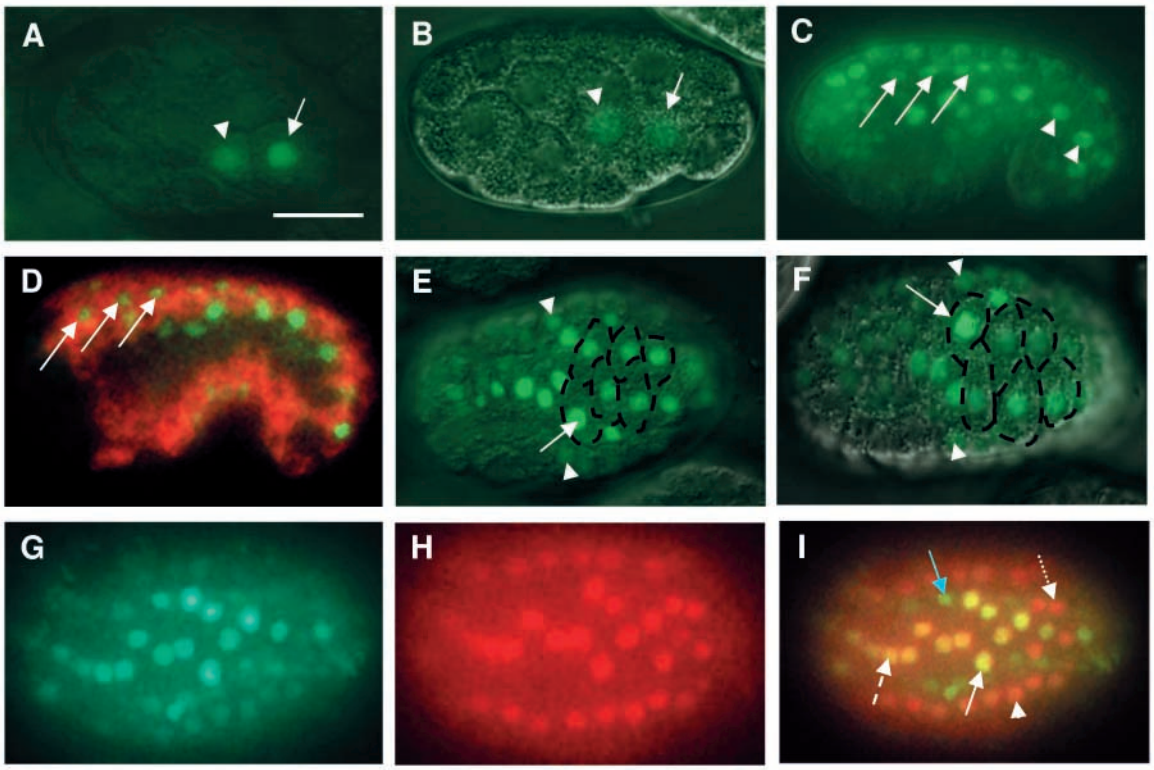

Fig. 5. Embryonic expression of *tbx-8* and *tbx-9* reporters. The earliest detectable *tbx-8::GFP* and *tbx-9::GFP* expression is seen in the nuclei of the gut cell precursors Ea and Ep at the onset of gastrulation, around 100 minutes following first cleavage (A-B). Ea and Ep are moving dorsally, into the interior. (A) TBX-8::GFP (Ea, arrowhead, Ep, arrow), (B) TBX-9::GFP (Ea, arrowhead, Ep, arrow). *tbx-8* and *tbx-9* are subsequently expressed in muscle and hypodermal cells. (C) Expression of *tbx-8::GFP* in dorsal muscle cells (arrows) and lateral hypodermal cells (arrowheads) at the 1.5-fold stage. To confirm these cells types, co-staining was performed with muscle and hypodermal specific markers. (D) TBX-9 stained green with a GFP antibody. The outlines of muscles cells are stained red with the muscle antibody NE8/4C6.3 and dorsal muscle cells expressing *tbx-9* are indicated (arrows). Similar results were obtained for TBX-8 (data not shown). (E-I) Hypodermal expression of *tbx-8::GFP* and *tbx-9::GFP*. TBX-8::GFP (E) and TBX-9::GFP (F) can be seen in the nuclei of dorsal hypodermal cells undergoing intercalation (around 300 minutes following first cleavage). The expression is particularly strong in cells that are just starting to intercalate (E,F, arrows). Outlines of cells undergoing the early stages of intercalation are shown with a black dotted line. Weaker expression can also be seen in lateral hypodermal cells (E,F, arrowheads). (G-I) Embryo co-stained with antibodies to show TBX-9::GFP in green and LIN-26 (expressed in all hypodermal cells) in red. (G) Green channel only showing cells expressing TBX-9::GFP stained with a GFP antibody. (H) Red channel only showing cells expressing LIN-26. (I) Merged image. Yellow nuclei strongly expressing both LIN-26 and TBX-9 can be seen in dorsal hypodermal cells that are beginning to intercalate (white solid arrow). Once cells are intercalated at the anterior TBX-9 expression is weaker and nuclei appear orange-yellow (dashed arrow). Cells at the posterior that have yet to intercalate express TBX-9 very weakly in this embryo and the nuclei appear orange-red (dotted arrow). Weak TBX-9 expression can also be seen in lateral hypodermal cells, in which the nuclei appear orange (arrowhead). Ventral hypodermal cells (not visible in this focal plane), which express LIN-26 but not TBX-9, stained red (not shown). Underlying muscle cell nuclei, which express TBX-9 but not LIN-26, appear green (blue arrow). Similar results were obtained with a *tbx-8::GFP* reporter. Posterior is to the right in all panels. Scale bar, 10 μm.

lateral hypodermal cells during dorsal intercalation (Fig. 5E-G), although expression in lateral hypodermal cells at this stage was weaker. Expression in lateral hypodermal (seam) cells could also be seen later in embryogenesis until the 1.5-fold stage (Fig. 5C). No expression of either *tbx-8* or *tbx-9* was observed in ventral hypodermal cells. The earliest detectable muscle cell expression of *tbx-8* and *tbx-9* was seen around the 400-cell stage, when muscle cells were present as two rows on the left and right sides of the embryo (Fig. 6A-B). Expression of *tbx-8* and *tbx-9* in hypodermal and muscle cells around the time when defects in these two cell types are first observed supports the view that hypodermal and muscle defects in *tbx-8*/*tbx-9(RNAi)* animals are likely to be largely cell autonomous, rather than one being a consequence of the other.

tbx-8 and *tbx-9* activate *vab-7* expression in muscle and hypodermal cells

vab-7 is required for the correct patterning of posterior body muscles and hypodermis and is expressed in posterior body muscle precursors and in hypodermal cells (Ahringer, 1996). The similarity in phenotype between *vab-7* mutants and *tbx-9(RNAi)* animals, and the overlapping expression domains of *vab-7*, *tbx-8* and *tbx-9* (Fig. 6A-C) (Ahringer, 1996), suggest a possible regulatory interaction. To investigate this, we asked whether RNAi silencing of *tbx-8* and *tbx-9* affects the expression pattern of a *vab-7::GFP* reporter. Muscle expression of *vab-7::GFP* was abolished in these embryos, indicating that *tbx-8* and *tbx-9* function to promote muscle expression of *vab-7*, either directly or indirectly (Fig. 6E, compared with Fig. 6D). At the comma stage, *vab-7::GFP* is

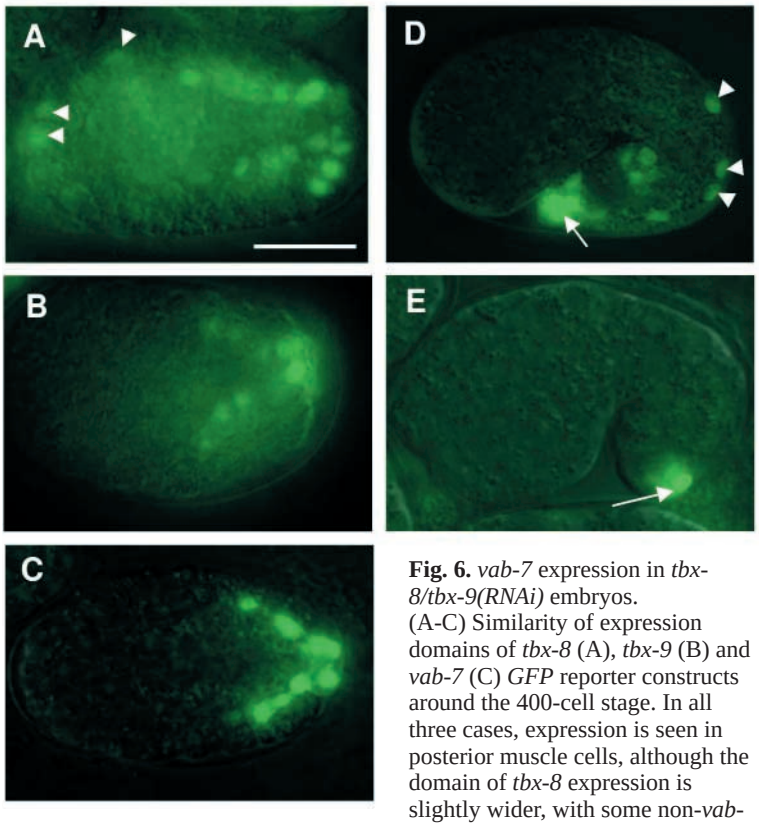

Fig. 6. *vab-7* expression in *tbx-8/tbx-9(RNAi)* embryos. (A-C) Similarity of expression domains of *tbx-8* (A), *tbx-9* (B) and *vab-7* (C) *GFP* reporter constructs around the 400-cell stage. In all three cases, expression is seen in posterior muscle cells, although the domain of *tbx-8* expression is slightly wider, with some non-*vab*-7-expressing nuclei showing up (A, arrowheads). (D) *vab*-7::*GFP* expressing nuclei at the 1.5-fold stage. Expression is seen in posterior muscle cells (arrowheads), the majority of which are dorsal, and in the posterior hypodermal cells hyp 8-11 (arrow, 4-5 nuclei). The *vab-7::GFP* construct gives a similar expression pattern to the *vab-7::lacZ* construct and antibody staining previously reported (Esmaeili et al., 2002; Ahringer, 1996). (E) *vab*-7::GFP expression in *tbx-8/tbx-9(RNAi)* embryos at the same stage. No muscle-specific expression of *vab*-7 is observed, even though the same number of muscle cells are present (see text). *vab*-7 expression is still seen in one or two posterior hypodermal cells (arrow), which appear to have shifted slightly anteriorly, presumably due to the general disorganisation of *tbx-8/tbx-9(RNAi)* embryos. Posterior is to the right. Scale bar, 10 μm.

normally expressed in four to five posterior hypodermal nuclei (4.7±0.1, *n*=18) (Fig. 6D) (Esmaeili et al., 2002), but in *tbx-8/9(RNAi)* embryos expression was seen in only one or two posterior hypodermal nuclei (1.7±0.1, *n*=13, Fig. 6E). Silencing either *tbx-8* or *tbx-9* alone did not significantly reduce *vab-7* expression (data not shown), indicating that these two genes have redundant roles in *vab-7* activation. It is possible, however, that the low penetrance *vab-7*-like bobbed-tail phenotype in *tbx-9(RNAi)* animals is the result of a slight reduction of *vab-7* expression in posterior hypodermis not detectable with the reporter.

Overexpression of either *tbx-8* or *tbx-9* drives ectopic *vab-7* expression

To see if *tbx-8* and *tbx-9* are sufficient for *vab-7* expression, we generated transgenic worms in which either *tbx-8* or *tbx-9* expression was driven by two strong inducible heat-shock promoters *hsp16-2 and hsp-16-41*, in addition to carrying a *vab-7*::*GFP* reporter construct (see Materials and methods). Following heat treatment, ectopic *vab-7::GFP* expression driven by either TBX-8 or TBX-9 could be observed up to the 400-cell stage of embryogenesis (Fig. 7A-D). No ectopic *vab-7* expression was seen as a result of heat treatment in the absence of the *tbx-8* or *tbx-9* heat-shock constructs (Fig. 7E-F). Therefore, *tbx-8* and *tbx-9* are both necessary and sufficient for *vab-7* expression in embryos.

Do TBX-8/TBX-9 activate *vab-7* directly?

An obvious question is whether or not the activation of *vab-7* expression by *tbx-8/tbx-9* is direct. All T-box proteins analysed so far interact with a characteristic DNA binding site in target genes with the core consensus sequence GGTGTGAA (reviewed by Papaioannou, 2001; Smith, 1999). The *vab-7* 5′ regulatory region contains two close-match T-box binding sites situated close together, ~2 kb from the start of transcription (Fig. 8A). As these sites are good candidates for TBX8/9 binding, we engineered a *vab-7::GFP* reporter construct in which both sites were mutated. We found, however, that the posterior muscle and hypodermal expression pattern of *vab-7* was unchanged in transgenic embryos carrying the mutated *vab-7::GFP* reporter (Fig. 8B,D,F). This suggests either that TBX-8 and TBX-9 do not regulate *vab-7* directly, or that TBX-8/9 do activate *vab-7* directly, but bind to alternative or additional binding sites, perhaps with a more degenerate sequence. T-box proteins in other organisms have been found to exhibit complex binding interactions with in-vivo target sites, often with a high degree of redundancy (Kusch et al., 2002; reviewed by Papaioannou, 2001).

T-box mediated anterior repression of *vab-7*

Although posterior expression of *vab-7* was unchanged by mutating the two putative T-box binding sites, we did detect a marked difference in *vab-7* expression at the anterior of embryos carrying the mutated reporter. Normally, no *vab-7* expression is observable in the anterior of embryos at any stage of development (Ahringer, 1996) (this report). In transgenic lines carrying the mutated *vab-7* reporter, however, significant anterior *vab-7* expression is reproducibly seen (77% of embryos, *n*=48), at several different embryonic stages (Fig. 8B,D,F). This raises the possibility that there is a T-box factor in *C. elegans* that represses *vab-7* expression in the anterior of embryos and that this factor normally binds directly to the T-box sites we have mutated. In order to investigate this, we silenced each of the remaining 18 T-box genes singly by RNAi and monitored the effect on wild-type *vab-7* expression. We found that silencing *tbx-30* (*Y59E9AR.3*) resulted in comparable ectopic anterior expression of *vab-7::GFP* (Fig. 8C,E,G), thereby phenocopying the effect of mutating the T-box binding sites in the *vab-7* reporter. There were no obvious morphological phenotypes associated with silencing *tbx-30*. Silencing the other 17 *C. elegans* T-box genes had no effect on *vab-7::GFP* expression (data not shown). Thus, *tbx-30* encodes a novel, anterior repressor of *vab-7*. Examination of the amino acid sequences of TBX-8, TBX-9 and TBX-30 revealed that there are highly acidic domains at the C-termini of TBX-8 and TBX-9 (data not shown), consistent with a role for these two

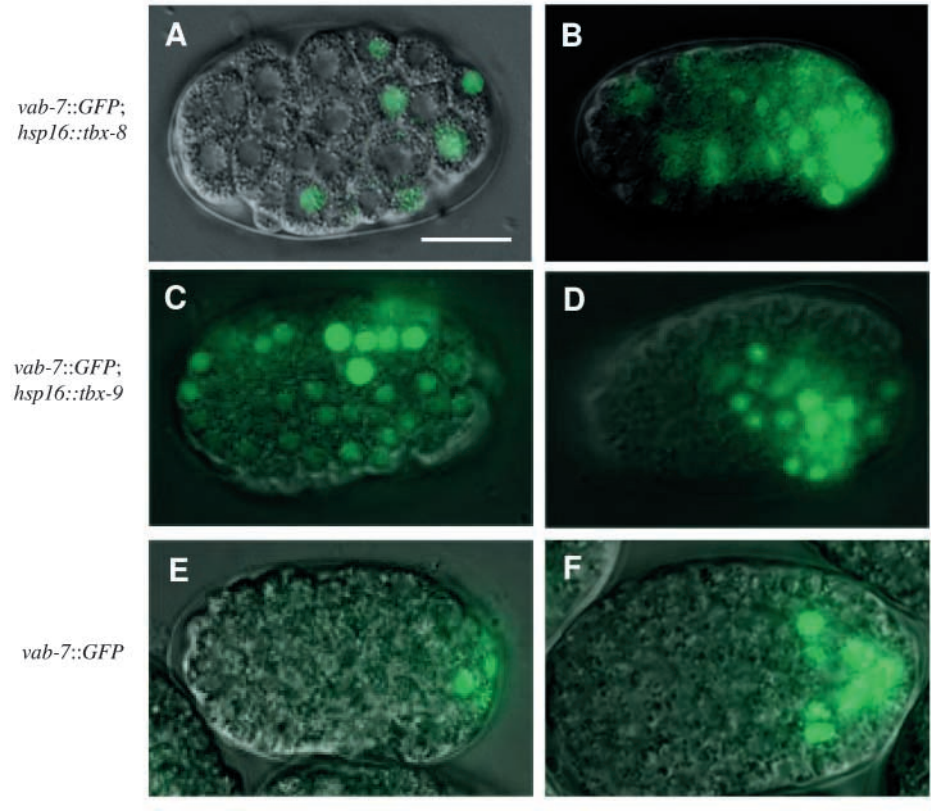

Fig. 7. Expression of *vab-7* in embryos overexpressing *tbx-8* or *tbx-9*. Expression of *vab-7::GFP* was monitored in worms that also carried integrated *hsp16-2::tbx-8 + hsp16-41::tbx-8* or *hsp16-2::tbx-9 + hsp16-41::tbx-9* constructs in which high level expression of *tbx-8* or *tbx-9* could be ubiquitously induced by heat treatment. (A-B) Following heat-shock induction of *tbx-8* at 33°C for 45 minutes and a subsequent incubation at 20°C for 2 hours, ectopic *vab*-7::GFP expression can be seen up to the 400-cell stage. (A) Early embryos; (B) later embryos around the 400-cell stage. (C-D) Similar results were obtained following heat shock induction of *tbx-9*, using the same heat treatment conditions. (E-F) *vab-7::GFP* embryos that do not contain the *hsp16::tbx-8* or *hsp16::tbx-9* constructs, subject to the same heat treatment regime. VAB-7 is seen in very few posterior cells around the 200-cell stage (E), and in muscle cells around the 400-cell stage, as has been previously reported (Ahringer, 1996) (this report). Posterior is to the right in all panels. Scale bar, 10 μm.

genes in transcriptional activation. No such activation domain is present in TBX-30, however, as we would expect for a transcriptional repressor.

VAB-7 represses *mab-9* expression in posterior cells

In a separate screen for genes that regulate the expression of the T-box gene *mab-9* (Pocock and Woollard, unpublished observations), we found that *mab-9* expression was altered in a *vab-7* mutant background. *mab-9* is normally first expressed in embryos at the 1.5-fold stage in the nuclei of three cells around the presumptive rectum, B, F and one hyp 7 nucleus (Fig. 9B) (Woollard and Hodgkin, 2000). In a *vab-7(e1562)* mutant background, however, the domain of *mab-9* expression was more extensive, with three to four extra *mab-9* expressing nuclei appearing more posterior to the usual *mab-9* expressing nuclei (Fig. 9D). It is difficult to unambiguously assign these nuclei in a *vab-7* background, because of the disruption in normal cell positioning in this mutant, but they appear to be muscle nuclei, and would normally be expected to express *vab-7*. We examined *mab-9* expression in *tbx-8/tbx-9(RNAi)* embryos and found similar ectopic posterior expression (data not shown). This is consistent with the notion that TBX-8 and TBX-9 are required for the expression of *vab-7* in posterior muscle cells, and that VAB-7 is required, in turn, to repress *mab-9* expression in these cells.

Discussion

Our data suggest that *tbx-8* and *tbx-9* have crucial, overlapping roles in controlling several aspects of embryonic morphogenesis and patterning. These two genes are required for the correct arrangement of dorsal and lateral hypodermal cells during intercalation and elongation and also form part of a regulatory network that includes two other T-box genes, *tbx-30* and *mab-9*, and the homeobox gene *vab-7*. This network of T-box genes and *vab-7* is important for the correct patterning of posterior cells.

Role of *tbx-8* and *tbx-9* in embryonic hypodermal morphogenesis

Embryos lacking both *tbx-8* and *tbx-9* fail to complete dorsal hypodermal intercalation, arresting as late embryos or short L1 larvae with gross morphological defects. Consistent with this phenotype, we found that *tbx-8* and *tbx-9* were both expressed at high levels in dorsal hypodermal cells undergoing intercalation, suggesting that *tbx-8*/*tbx-9* are likely to be acting cell autonomously within the dorsal hypodermis to control these rearrangements. Although no obvious defect was seen on the ventral side of embryos during enclosure, the lateral hypodermal (seam) cells were often mispositioned, or pinched out of line. This may be a consequence of the dorsal intercalation defect, with the seam cells not being held in line properly by the dorsal syncytium.

There are some known mutants in *C. elegans* with similar dorsal hypodermal phenotypes, which might point to biochemical pathways in which *tbx-8 and tbx-9* are acting. For instance, *die-1* (*d*orsal *i*ntercalation and *e*longation defective) mutants also initiate, but fail to complete, dorsal intercalation (Heid et al., 2001). *tbx-8*, *tbx-9* and *die-1* are all expressed within dorsal hypodermal cells undergoing intercalation (Heid et al., 2001 and this report). *die-1* encodes a zinc finger protein thought to act as a transcriptional regulator, although it is not known at present what the transcriptional targets of *die-1* might be, or how this gene might be regulated. It is also noteworthy

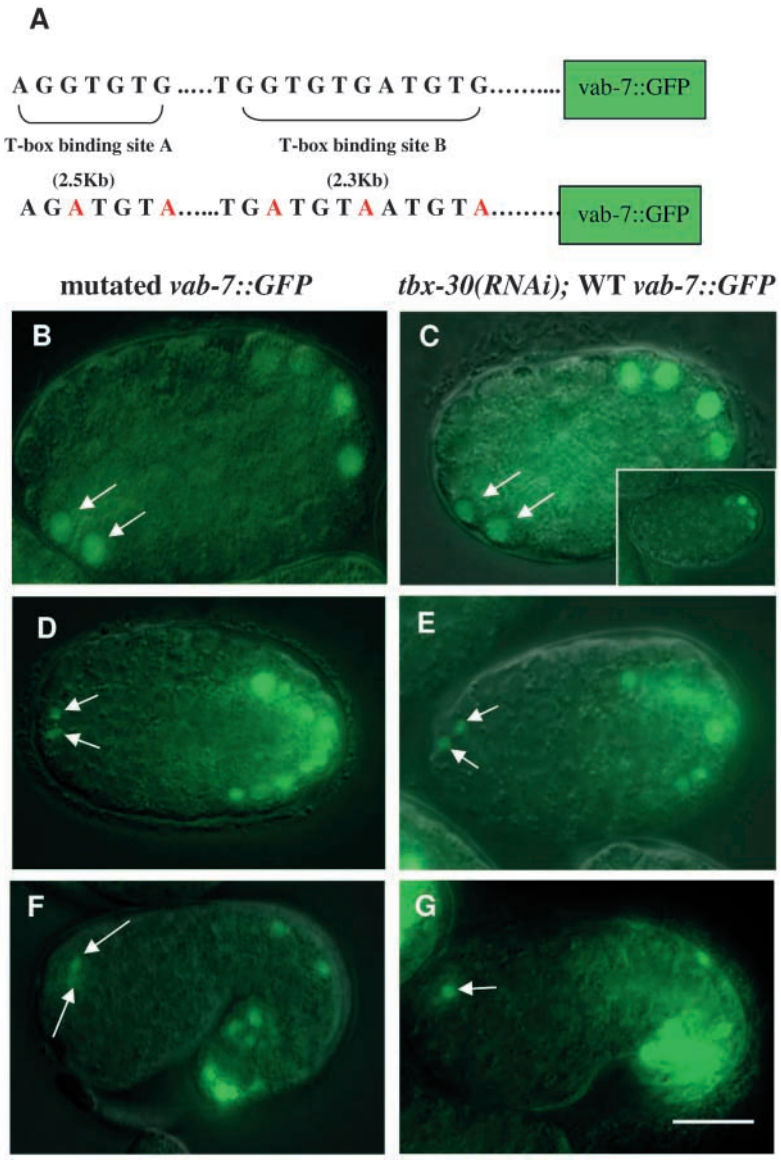

Fig. 8. T-box mediated anterior repression of *vab-7*. (A) Upper line, schematic of *vab-7* 5′ regulatory region of *vab-7::GFP* construct showing putative T-box binding sites A and B. Lower line, sequence of mutated sites A and B, following site directed mutagenesis. These mutated sites would not be expected to bind T-box proteins (Sinha et al., 2000). (B,D,F) Expression of *vab-7::GFP* in transgenic animals carrying this mutated construct. The normal posterior pattern of *vab-7::GFP* expression can be seen, together with ectopic expression at the anterior. (B) Ectopic anterior expression can be seen at around the 100-cell stage (arrows). The inset panel in (C) shows WT *vab-7::GFP* expression in four posterior Cxxp cells at the same stage, for comparison. Note there is no anterior expression in this case. (D) Ectopic anterior expression around the 400-cell stage (arrows) together with the usual posterior muscle expression of *vab-7::GFP* seen at this stage. (F) Ectopic expression at the anterior at the 1.5-fold stage (arrows) together with the usual posterior muscle and hypodermal VAB-7::GFP observable at this stage. (C,E,G) expression of WT, non-mutated *vab-7::GFP* in *tbx-30(RNAi)* embryos. Ectopic expression of *vab-7* is observable in the same anterior cells at comparable stages to the T-box binding site-mutated *vab-7* reporter, suggesting that TBX-30 normally represses *vab-7* expression at the anterior of embryos by binding to these sites. (C) Ectopic expression of *vab-7* around the 100-cell stage in the same cells as in (B) (arrows). The inset panel shows WT *vab-7::GFP* expression at the same stage, for comparison. (E) Ectopic anterior expression around the 400-cell stage (arrows), comparable to that seen in (D). (G) Ectopic anterior expression at the 1.5-fold stage, comparable to that seen in (F). The usual posterior *vab-7* expression pattern is seen in all cases (slightly out of focus in (G)) Posterior is to the right, dorsal is up in panels (B-G). Scale bar, 10 μm.

that *tbx-8/tbx-9(RNAi)* animals display other phenotypes in common with *die-1* mutants. These include lateral hypodermal cells being pinched out of line, body wall muscle cell positioning defects and abnormalities in gut morphogenesis (Heid et al., 2001) (this report). This would support the idea that *tbx-8/tbx-9* and *die-1* may act in the same pathway to regulate several aspects of embryonic morphogenesis.

Dorsal hypodermal intercalation in *C. elegans* has been likened to the process of convergent extension (directed intercalation of cells towards an axis of extension) in vertebrates (Chin-Sang and Chisholm, 2000). Intriguingly, it has been reported that the T-box gene *spadetail* is required in zebrafish embryos for lateral mesoderm cells to undergo the convergent extension movements of gastrulation (Griffin et al., 1998; Ho and Kane, 1990). Furthermore, *Brachyury* in *Xenopus* has also been shown to be required for convergent extension movements (Conlon et al., 1996; Conlon and Smith, 1999). Therefore, it seems that regulation of cell intercalation movements during embryonic morphogenesis is a conserved T-box gene function. Since *spadetail* and *Brachyury* have no obvious counterparts in *C. elegans*, and *tbx-8* and *tbx*-9 have no obvious counterparts in vertebrates, we suggest that this may be an ancient role, with its origin in a common ancestral gene.

TBX-8/TBX-9 mediated activation of *vab-7*

We have shown that: (1) *tbx-8*, *tbx-9* and *vab-7* have overlapping expression domains in embryos in posterior muscle and hypodermal cells; (2) *vab-7* expression in embryos requires *tbx-8/tbx-9* activity; and (3) overexpression of *tbx-8* or *tbx-9* is sufficient to drive ectopic *vab-7* expression throughout the embryo. This suggests that *tbx-8*, *tbx-9* and *vab-7* function in a common genetic pathway to control embryonic patterning events, with *tbx-8* and *tbx-9* acting as upstream activators of *vab-7*.

Posterior muscles (those derived from the C blastomere) in *vab-7* mutants are disorganised. Muscle cells are often bunched together laterally or even form rings with neighbouring rows

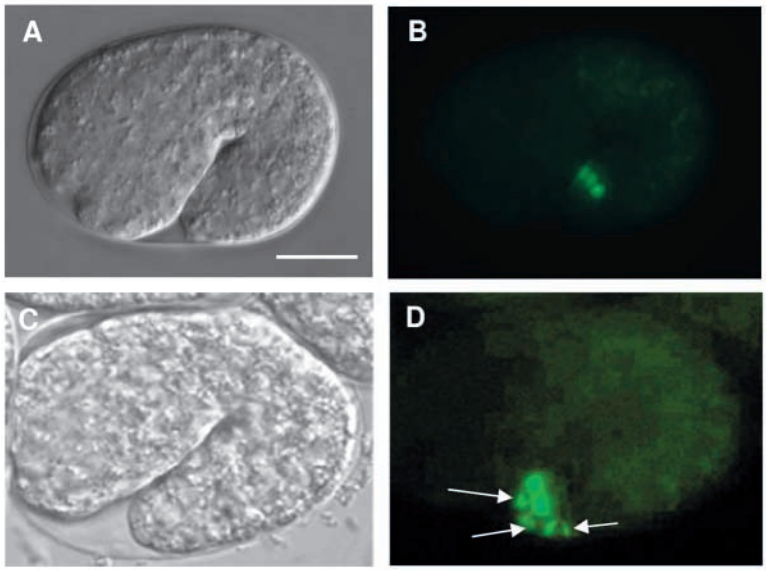

Fig. 9. MAB-9 localisation in *vab-7* mutants. (A,B) Embryo at the 1.5-fold stage carrying an integrated *mab-9::GFP* translational reporter construct (nomarski image on the left, (A), corresponding fluorescence image on the right, (B)). MAB-9 can be seen in three nuclei at this stage around the presumptive rectum, B, F and hyp 7, as has been previously reported (Woollard and Hodgkin, 2000). (C,D) *vab-7(e1562)* embryo also carrying an integrated *mab-9::GFP* reporter at the same stage (nomarski image on the left, (C), fluorescence image on the right, (D)). Ectopic MAB-9 can be seen in more posterior nuclei (arrows). Posterior is to the right in all panels. Scale bar, 10 μm.

(Ahringer, 1996). We found similar defects in *tbx-8*/*tbx-9(RNAi)* animals, with muscle cells being present in the correct number, but severely misplaced, consistent with the notion that *tbx-8* and *tbx-9* are required for *vab-7* expression and subsequent patterning activity in C blastomere-derived muscle cells. The muscle defects seen in *tbx-8*/*tbx-9(RNAi)* animals were not confined to the posterior, however, so it is likely that there are other muscle-specific targets of *tbx-8*/*tbx-9* besides *vab-7*. It is also possible that some of the muscle defects seen in *tbx-8*/*tbx-9(RNAi)* animals are a secondary consequence of the other morphogenetic abnormalities. The bobbed tail appearance of *tbx-9(RNAi)* and *vab-7(e1562)* animals is likely to be the outcome of a hypodermal defect that is common to both situations. However, *tbx-8/tbx-9(RNAi)* worms also have more severe hypodermal defects during dorsal intercalation that are not seen in *vab-7* mutants, suggesting that TBX-8 and TBX-9 are likely to influence the expression of multiple target genes involved in hypodermal cell rearrangements as embryogenesis proceeds.

Overexpression of *tbx-8* or *tbx-9* from the strong, inducible heat-shock promoter is sufficient to drive ectopic *vab-7* expression throughout the embryo. The *caudal* orthologue *pal-1* has also been shown to be capable of driving ectopic *vab-7* expression, and, like *tbx-8*/*tbx-9*, is required for *vab-7* expression (Ahringer, 1997). It is therefore of interest to consider whether *tbx-8*/*tbx-9* act in the same pathway as *pal-1* to regulate *vab-7* expression. We have performed experiments, however, that show that *tbx-8* and *tbx-9* were still expressed in *pal-1(RNAi)* embryos (data not shown), albeit in a disorganised pattern, as would be expected if *pal-1* expression was silenced (Hunter and Kenyon, 1996). Likewise, *pal-1::GFP* is still expressed in *tbx-8*/*tbx-9(RNAi)* embryos (data not shown); therefore we conclude that *tbx-8*/*tbx-9* and *pal-1* probably act in separate, complementary pathways to regulate *vab-7* expression.

The activation of *evenskipped* in posterior cells by T-box genes has been reported in other systems, suggesting that this may be a conserved mechanism for controlling posterior pattern formation. For example, *brachyenteron* is required for *eve* expression in the hindgut and anal pad primordia of *Drosophila* (Kusch and Reuter, 1999; Singer et al., 1996), and in mouse, *evx-1* expression has been shown to be dependent on *Brachyury* in the posterior tail bud (Rashbass et al., 1994). Likewise, *no tail* (*ntl*-zebrafish *Brachyury*) is required for the maintenance of *eve1* expression during tail extension in zebrafish (Joly et al., 1993). Whether these examples of T-box gene mediated regulation of *eve* genes involve direct or indirect effects remains to be seen. It is also noteworthy that ectopic *Xbra* expression in *Xenopus* causes marked induction of the *eve* homologue *Xhox3* (Cunliffe and Smith, 1992), similar to the induction of *vab-7* expression caused by *tbx-8* or *tbx-9* overexpression reported here. Perhaps the regulation of *eve* has been taken over by *tbx-8/tbx-9* in *C. elegans* in the absence of a bona fide *Brachyury* homologue.

TBX-30 is likely to be a direct repressor of *vab-7* expression in anterior cells

If *tbx-8* and *tbx-9* directly activate *vab-7*, then this is not through the two T-box binding sites we have described, as mutating these sites did not eliminate *vab-7* expression. By contrast, we found that mutating these T-box binding sites caused ectopic anterior expression of *vab-7*, suggesting that *vab-7* may be subject to direct inhibitory regulation by another T-box gene. T-box genes have been shown to act as either activators or inhibitors of target gene expression (reviewed by

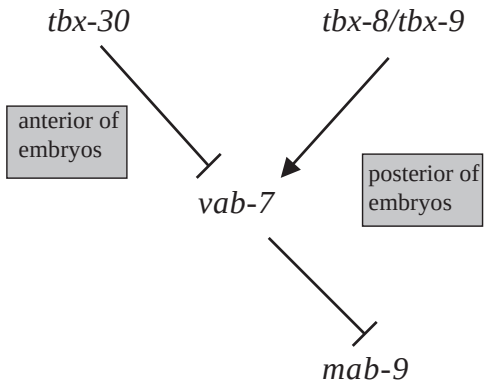

Fig. 10. Interactions between T-box genes and *vab-7* in *C. elegans*. *vab-7* expression is activated (probably indirectly) at the posterior of embryos by TBX-8 and TBX-9 working together. VAB-7, in turn, functions to repress *mab-9* expression in posterior cells. Meanwhile, at the anterior of embryos, *vab-7* is itself repressed by the action of TBX-30. This repression is likely to be direct, acting through T-box binding sites in the *vab-7* 5′ regulatory region.

Papaioannou, 2001). By silencing each of the *C. elegans* T-box genes in turn, we found that *tbx-30* normally repressed *vab-7* expression in anterior cells during embryogenesis. *tbx-30* probably directly represses *vab-7* at the anterior, through the T-box binding sites we have defined, as mutating these binding sites had exactly the same effect on *vab-7* expression as silencing *tbx-30*.

Inhibitory effects of VAB-7 on *mab-9* expression

eve orthologues are known to function as transcriptional repressors in a wide variety of situations and are thought to act by interacting with the basal transcriptional machinery at specific promoters (Han and Manley, 1993; Li and Manley, 1998). The VAB-7 protein contains two putative repressor domains that are also found in other members of the *eve* family. There is a polyalanine stretch near the N-terminus of VAB-7 and a region rich in proline and serine residues at the C-terminus (Ahringer, 1996). Alanine-rich and proline-rich regions have both been shown to function in transcriptional repression (Um et al., 1995). Our data suggest that VAB-7 acts to repress *mab-9* expression in cells at the very posterior of embryos at the 1.5-fold stage. Ectopic expression of *mab-9* is generally deleterious during development, resulting in embryonic arrest or animals with posterior deformations (Woollard and Hodgkin, 2000). It is possible, therefore, that inappropriate, ectopic expression of *mab-9* in posterior cells contributes to the abnormal posterior phenotype of *vab-7* mutant animals.

Overall, we have described a situation in which the activities of at least four different T-box genes in *C. elegans* (*tbx-8*, *tbx-9*, *tbx-30* and *mab-9*) are linked by *vab-7*. A model for these regulatory interactions is depicted in Fig. 10. Although positive regulation of *eve* homeobox genes by T-box proteins has been reported in other systems, this is the first demonstration that an *eve* homeobox gene is also sensitive to T-box mediated repression, and that T-box genes themselves can be subject to repression by *eve*. The potential evolutionary association between the role of *tbx-8* and *tbx-9* in dorsal hypodermal intercalation in *C. elegans* and the role of T-box genes in convergent extension movements of cells in other organisms is a second intriguing connection. Perhaps the involvement of T-box genes in these kinds of cell rearrangements, which are an essential prelude to metazoan morphogenesis, will turn out to be widespread.

We would like to thank Jonathan Hodgkin and Sarah Newbury for helpful comments on the manuscript. R.P. and A.W. were funded by the UK Medical Research Council, the Biotechnology and Biological Sciences Research Council, and the Royal Society. M.M. and J.A. were funded by Wellcome Trust Fellowships (Nos 054523 and 045515). We would also like to thank Behrooz Esmaeili (University of Oxford) for making the *vab-7::GFP* reporter construct used in this study.

References

Ahringer, J. (1996). Posterior patterning by the *Caenorhabditis elegans even-skipped* homolog *vab-7*. *Genes Dev*. **10**, 1120-1130.

Ahringer, J. (1997). Maternal control of a zygotic patterning gene in *Caenorhabditis elegans*. *Development* **124**, 3865-3869.

Bamshad, M., Le, T., Watkins, W. S., Dixon, M. E., Kramer, B. E., Roeder, A. D., Carey, J. C., Root, S., Schinzel, A., Van Maldergem, L. et al. (1999). The spectrum of mutations in *TBX3*: genotype/phenotype relationship in ulnar-mammary syndrome. *Am. J. Hum. Genet*. **64**, 1550-1562.

Basson, C. T., Huang, T., Lin, R. C., Bachinsky, D. R., Weremowicz, S., Vaglio, A., Bruzzone, R., Quadrelli, R., Lerone, M., Romeo, G. et al. (1999). Different *TBX5* interactions in heart and limb defined by Holt-Oram syndrome mutations. *Proc. Natl. Acad. Sci. USA* **96**, 2919-2924.

Braybrook, C., Doudney, K., Marcano, A. C., Arnason, A., Bjornsson, A., Patton, M. A., Goodfellow, P. J., Moore, G. E. and Stanier, P. (2001). The T-box transcription factor gene *TBX22* is mutated in X-linked cleft palate and ankyloglossia. *Nat. Genet*. **29**, 179-183.

Brown, S. J., Parrish, J. K., Beeman, R. W. and Denell, R. E. (1997). Molecular characterization and embryonic expression of the *even-skipped* ortholog of *Tribolium castaneum*. *Mech. Dev*. **61**, 165-173.

Chapman, D. L. and Papaioannou, V. E. (1998). Three neural tubes in mouse embryos with mutations in the T-box gene Tbx6. *Nature* **391**, 695-697.

Chin-Sang, I. D. and Chisholm, A. D. (2000). Form of the worm: genetics of epidermal morphogenesis in *C. elegans*. *Trends Genet*. **16**, 544-551.

Conlon, F. L. and Smith, J. C. (1999). Interference with *brachyury* function inhibits convergent extension, causes apoptosis, and reveals separate requirements in the FGF and activin signalling pathways. *Dev. Biol*. **213**, 85-100.

Conlon, F. L., Sedgwick, S. G., Weston, K. M. and Smith, J. C. (1996). Inhibition of *Xbra* transcription activation causes defects in mesodermal patterning and reveals autoregulation of *Xbra* in dorsal mesoderm. *Development* **122**, 2427-2435.

Cunliffe, V. and Smith, J. C. (1992). Ectopic mesoderm formation in Xenopus embryos caused by widespread expression of a *Brachyury* homologue. *Nature* **358**, 427-430.

Esmaeili, B., Ross, J., Neades, C., Miller, D. M. III and Ahringer, J. (2002). The *C. elegans even-skipped* homologue, *vab-7*, specifies DB motoneurone identity and axon trajectory. *Development* **129**, 853-862.

Fire, A., Xu, S., Montgomery, M. K., Kostas, S. A., Driver, S. E. and Mello, C. C. (1998). Potent and specific genetic interference by double-stranded RNA in *Caenorhabditis elegans*. *Nature* **391**, 806-811.

Goh, P.-Y. and Bogaert, T. (1991). Positioning and maintenance of embryonic body wall muscle attachments in *C. elegans* requires the *mup-1* gene. *Development* **111**, 667-681.

Griffin, K. J., Amacher, S. L., Kimmel, C. B. and Kimelman, D. (1998). Molecular identification of spadetail: regulation of zebrafish trunk and tail mesoderm formation by T-box genes. *Development* **125**, 3379-3388.

Han, K. and Manley, J. L. (1993). Transcriptional repression by the Drosophila *even-skipped* protein: definition of a minimal repression domain. *Genes Dev*. **7**, 491-503.

Heid, P. J., Raich, W. B., Smith, R., Mohler, W. A., Simokat, K., Gendreau, S. B., Rothman, J. H. and Hardin, J. (2001). The zinc finger protein DIE-1 is required for late events during epithelial cell rearrangement in *C. elegans*. *Dev. Biol*. **236**, 165-180.

Herrmann, B. G. (1995). The mouse *Brachyury (T)* gene. *Semin. Dev. Biol*. **6**, 385-394.

Ho, R. K. and Kane, D. A. (1990). Cell-autonomous action of zebrafish *spt-1* mutation in specific mesodermal precursors. *Nature* **348**, 728-730.

Huang, X., Cheng, H. J., Tessier-Lavigne, M. and Jin, Y. (2002). MAX-1, a novel PH/MyTH4/FERM domain cytoplasmic protein implicated in netrin-mediated axon repulsion. *Neuron* **34**, 563-576.

Hunter, C. P. and Kenyon, C. (1996). Spatial and temporal controls target PAL-1 blastomere specification activity to a single blastomere lineage in *C. elegans* embryos. *Cell* **87**, 217-226.

Joly, J. S., Joly, C., Schulte-Merker, S., Boulekbache, H. and Condamine, H. (1993). The ventral and posterior expression of the zebrafish homeobox gene eve1 is perturbed in dorsalized and mutant embryos. *Development* **119**, 1261-1275.

Kispert, A., Herrmann, B. G., Leptin, M. and Reuter, R. (1994). Homologs of the mouse *Brachyury* gene are involved in the specification of posterior terminal structures in Drosophila, Tribolium, and Locusta. *Genes Dev*. **8**, 2137-2150.

Kispert, A., Koschorz, B. and Herrmann, B. G. (1995). The T protein encoded by *Brachyury* is a tissue-specific transcription factor. *EMBO J*. **14**, 4763-4772.

Kofron, M., Demel, T., Xanthos, J., Lohr, J., Sun, B., Sive, H., Osada, S., Wright, C., Wylie, C. and Heasman, J. (1999). Mesoderm induction in Xenopus is a zygotic event regulated by maternal *VegT* via *TGFbeta* growth factors. *Development* **126**, 5759-5770.

Kostas, S. A. and Fire, A. (2002). The T-box factor MLS-1 acts as a molecular switch during specification of nonstriated muscle in *C. elegans*. *Genes Dev*. **16**, 257-269.

Kusch, T. and Reuter, R. (1999). Functions for Drosophila *brachyenteron* and

forkhead in mesoderm specification and cell signalling. *Development* **126**, 3991-4003.

Kusch, T., Storck, T., Walldorf, U. and Reuter, R. (2002). Brachyury proteins regulate target genes through modular binding sites in a cooperative fashion. *Genes Dev*. **16**, 518-529.

Li, C. and Manley, J. L. (1998). *Even-skipped* represses transcription by binding TATA binding protein and blocking the TFIID-TATA box interaction. *Mol. Cell Biol*. **18**, 3771-3781.

Mello, C. and Fire, A. (1995). DNA Transformation. In *Caenorhabditis elegans*: *Modern Biological Analysis of an Organism*. Vol. 48 (ed. D. Shakes and H. Epstein), pp. 451-482. San Diego: Academic Press.

Mohler, W. A., Simske, J. S., Williams-Masson, E. M., Hardin, J. D. and White, J. G. (1998). Dynamics and ultrastructure of developmental cell fusions in the *Caenorhabditis elegans* hypodermis. *Curr. Biol*. **8**, 1087-1090.

Muller, C. W. and Herrmann, B. G. (1997). Crystallographic structure of the T domain-DNA complex of the Brachyury transcription factor. *Nature* **389**, 884-888.

Papaioannou, V. E. (2001). T-box genes in development: from hydra to humans. *Int. Rev. Cytol*. **207**, 1-70.

Pflugfelder, G. O. and Heisenberg, M. (1995). *Optomotor-blind* of *Drosophila melanogaster*: A neurogenetic approach to optic lobe development and optomotor behaviour. *Comp. Biochem. Physiol. A Physiol*. **110**, 185-202.

Rashbass, P., Wilson, V., Rosen, B. and Beddington, R. S. (1994). Alterations in gene expression during mesoderm formation and axial patterning in *Brachyury* (*T*) embryos. *Int. J. Dev. Biol.* **38**, 35-44.

Simmer, F., Tijsterman, M., Parrish, S., Koushika, S. P., Nonet, M. L., Fire, A., Ahringer, J. and Plasterk, R. H. (2002). Loss of the putative RNA-directed RNA polymerase RRF-3 makes *C. elegans* hypersensitive to RNAi. *Curr. Biol*. **12**, 1317-1319.

Simon, H.-G. (1999). T-box genes and the formation of vertebrate forelimb and hindlimb specific pattern. *Cell Tissue Res.* **296**, 57-66.

Simske, J. S. and Hardin, J. (2001). Getting into shape: epidermal morphogenesis in *Caenorhabditis elegans* embryos. *Bioessays* **23**, 12-23.

Singer, J. B., Harbecke, R., Kusch, T., Reuter, R. and Lengyel, J. A. (1996). Drosophila *brachyenteron* regulates gene activity and morphogenesis in the gut. *Development* **122**, 3707-3718.

Sinha, S., Abraham, S., Gronostajski, R. M. and Campbell, C. E. (2000). Differential DNA binding and transcription modulation by three T-box proteins, T, TBX1 and TBX2. *Gene* **258**, 15-29.

Smith, J. (1999). T-box genes: what they do and how they do it. *Trends Genet.* **15**, 154-158.

Sulston, J. and Hodgkin, J. (1988). Methods. In *The Nematode Caenorhabditis elegans* (ed. W. B. Wood), pp. 587-606. New York: Cold Spring Harbor Laboratory Press.

Um, M., Li, C. and Manley, J. L. (1995). The transcriptional repressor even-skipped interacts directly with TATA-binding protein. *Mol. Cell Biol*. **15**, 5007-5016.

Woollard, A. and Hodgkin, J. (2000). The *Caenorhabditis elegans* fate-determining gene *mab-9* encodes a T-box protein required to pattern the posterior hindgut. *Genes Dev*. **14**, 596-603.

Zhang, J., Houston, D. W., King, M. L., Payne, C., Wylie, C. and Heasman, J. (1998). The role of maternal VegT in establishing the primary germ layers in Xenopus embryos. *Cell* **94**, 515-524.